Biophysical Reviews and Letters

QUANTITATIVE STUDIES OF SUBDIFFUSION IN LIVING CELLS AND ACTIN NETWORKS

EMILIA-LAURA MUNTEANU[1]*, ANJA LEA OLSEN[1], IVA TOLIC-NØRRELYKKE[1]†
HENRIK FLYVBJERG[2], LENE ODDERSHEDE[1], AND KIRSTINE BERG-SØRENSEN[3‡]

1: The Niels Bohr Institute, Blegdamsvej 17, 2100 Copenhagen, Denmark
2:Biosystems Department and Danish Polymer Centre, Risø National Laboratory, P. O. box 49, 4000 Roskilde, Denmark
3:Department of Physics, Technical University of Denmark, Fysikvej, Building 309, 2800 Kgs. Lyngby, Denmark

Received September 29, 2006
Revised September 29, 2006

Optical tweezers are a versatile tool in biophysics and have matured from a tool of manipulation to a tool of precise measurements. We argue here that the data analysis with advantage can be developed to a level of sophistication that matches that of the instrument. We review methods of analysis of optical tweezers data, primarily based on the power spectra of time series of positions for trapped spherical objects. The majority of precise studies in the literature are performed on *in vitro* systems, whereas in the present work, an example of an *in vivo* system is presented for which precise power spectral analysis is both useful and necessary. The biological system is the cytoplasm of fission yeast, *Schizosaccharomyces pombe* in which we observe subdiffusion of lipid granules. In a search for the cause of subdiffusion, we chemically disrupt the actin network in the cytoplasm and further consider *in vitro* networks of filamenteous actin undergoing similar chemical disruption.

Keywords: Optical tweezers; in vivo biophysics; data analysis

1. Introduction

Since Arthur Ashkin first demonstrated that optical tweezers can "capture life"[1,a], optical tweezers have developed tremendously, from a tool of manipulation to a tool of very precise measurements. For a recent review article see Ref. 3. For the present paper it is sufficient to know that the trapping potential of the optical tweezers is, to a very good approximation, harmonic.

*Present address: FOM Institute for Atomic and Molecular Physics, Kruislaan 407 Amsterdam, The Netherlands
†Present address: Max Planck Institute for Molecular Cell Biology and Genetics, Pfotenhauerstr. 108, 01307 Dresden, Germany
‡kirstine.berg-sorensen@fysik.dtu.dk
[a]Amusingly described by Steven Chu in his Nobel Lecture, Ref. 2, p. 701.

The latest development of the instrumentation is towards better force resolution [4,5] and better spatial resolution [6,7,8]. The latter examples all apply a dual-optical trap geometry and reach a spatial resolution at the Å-level. Applicability of precise instrumentation has been demonstrated for a number of interesting *in vitro* systems already: It was needed in order to directly observe base-pair stepping by RNA polymerase [9] and has been important in testing new methods in non-equilibrium statistical mechanics [10,11,12].

In living systems, optical tweezers have been applied even in studies of single molecules, e.g., the mobility of a single membrane protein [13,14]. For the latter case, application of our precise tools of analysis have been demonstrated elsewhere [15,16]. Here, we describe another example where optical tweezers are applied merely as a tool of detection in investigations of the cytoplasm of a living cell. As we shall see, for this example precision in the analysis is needed for some of the conclusions drawn.

The paper is organized as follows: First, we explain the advantages of power spectral analysis over an analysis based directly on the time-series of positions, also when subdiffusion is the subject. Second, we describe briefly the biological system studied and concentrate this part of the paper on experimental results and their analysis. Finally, we discuss experiments in an *in vitro* system that mimics the actin-network of the living cell.

2. Methods of data analysis

The raw signal of almost any optical tweezers experiment is a measure of the time series of positions, $(x(t), y(t), z(t))$ of an object held in the optical trap. This object is often a microsphere of known size and optical properties, and it may, e.g., be coupled to a single molecule of interest, or embedded in a viscoelastic medium of interest. In most optical tweezers systems, position is detected either via a position sensitive photodetector or via a quadrant photodiode [3]. Typically, further analysis is based either directly on the time series of positions, or on their power spectra. Below, we briefly review these options with special emphasis on the power spectral analysis. For simplicity, we describe the analysis of one coordinate only, say, $x(t)$, as the coordinates are assumed independent.

2.1. *Direct analysis of time series of positions*

From a series of N consecutive measurements of the position, $x(t_i); i = 1, \ldots N; t_i = i\Delta t$, found with sampling frequency $f_{\text{sample}} = 1/\Delta t$, it is straightforward to extract the first and second moments, $\overline{x}$ and $\overline{x^2}$, where the bar denotes average over time, and it is useful to find the histogram of positions visited, for comparison with an expected distribution of positions, and to calculate the auto-correlation function, $G(t)$,

$$G(j\Delta t) = \overline{\left(x(t_i) - \langle x \rangle\right)\left(x(t_{i+j}) - \langle x \rangle\right)} \ , \tag{1}$$

where averaging is performed over the variable i. Standard results from statistics furnish the error bars on these experimental measures.

The association of any physical interpretation to $\overline{x}$, $\overline{x^2}$ and $G(t)$ depends on the system studied. Consider a model example of a dielectric bead, held in optical tweezers of spring constant κ, and moving in a liquid with constant friction γ. If the time series is sufficiently long that measured data corresponds to a system in equilibrium, $\overline{x}$ equals the position of the minimum of the trapping potential, and $\overline{x^2} - \overline{x}^2 = k_B T/\kappa$. If in addition Δt is large compared to the time scale of inertial effects, $G(t) = (\overline{x^2} - \overline{x}^2)\exp(-\kappa t/\gamma)$. Here, T is temperature and k_B is Boltzmann's constant. With this interpretation at hand, the optical tweezers equipment can be calibrated [17].

Another quantity of interest is the mean square displacement, MSD(t):

$$\mathrm{MSD}(n\Delta t) = \frac{1}{N-i}\sum_{i=1}^{N-i}(x(t_{i+n}) - x(t_i))^2 \ . \tag{2}$$

For our model example, $\mathrm{MSD}(t) = 2Dt$ where D is the diffusion coefficient of the bead, $D = k_B T/\gamma$. Again, standard results from statistics may be used to find the experimental error bars on MSD(t).

Now that we have described how the quantities above are evaluted, one can discuss how prone they are to known, systematic errors. Drift will influence $\overline{x}$ and $\overline{x^2} - \overline{x}^2$, with a tendency to increase the latter. Unless the drift is well characterized in other ways, there is no systematic way to account for it. Parasitic filtering by the position detection system [18,19,20,21] may influence both $\overline{x^2} - \overline{x}^2$, $G(t)$ and MSD(t), and is not easily accounted for either. Low-pass filtering causes a delay in the detection of positions. With power spectral analysis, both artefacts can be accounted for in a systematic manner, as we discuss below.

2.2. *Power spectral analysis*

The power spectrum is defined from the Fourier transformed of the position, $\tilde{x}_k$, with

$$\tilde{x}_k = \int_{-T_{\mathrm{msr}}/2}^{T_{\mathrm{msr}}/2} \mathrm{d}t\, e^{i2\pi f_k t} x(t) \ , \ f_k \equiv k/T_{\mathrm{msr}} \ , \ k \text{ integer}, \tag{3}$$

where T_{msr} is the total measurement time, $T_{\mathrm{msr}} = N\Delta t$. The experimental power spectrum is then calculated as

$$P_k^{(\mathrm{ex})} \equiv |\tilde{x}_k|^2/T_{\mathrm{msr}} \tag{4}$$

for $k > 0$. Further, the standard deviation on the experimental power spectrum, found as in Eq. (4), equals

$$\sigma(P_k^{(\mathrm{ex})}) = P_k \ , \tag{5}$$

with P_k being the expectation value of the power spectrum at frequency f_k [22],[b]. This relation is shown explicitly in Ref. 19 for our model example. For a smooth power spectrum, we suggest "blocking" [23] and/or windowing with a square windowing function [22] to achieve error reduction. Details of this procedure are discussed elsewhere [19].

2.2.1. *Experimental artefacts: Parasitic filtering and aliasing*

When comparing an experimental power spectrum to a theory for it, a number of experimental artefacts should be considered:

(i) Some position detection systems act as a low-pass filter and thus reduce the power spectrum at high frequencies [18,19,20,21]. Fortunately, in frequency space, low-pass filtering corresponds simply to a multiplicative factor [18]. Assume that the detection system is associated with an (unwanted) characteristic filter function $g^{(\mathrm{diode})}(f)$ and that further, the data acquisition system is characterized by a filter function $g^{(\mathrm{elec})}(f)$. Thereby, the theoretical power spectrum, $P^{(\mathrm{theory})}$, should be modified to

$$P^{(\mathrm{filtered})}(f) = P^{(\mathrm{theory})}(f)\, g^{(\mathrm{diode})}(f)\, g^{(\mathrm{elec})}(f) \tag{6}$$

before comparing to the experimental data. For the detection system and frequency range applied below, the relevant filter characteristics is given in Eq. (G1) of Ref. 19, $g^{(\mathrm{diode})}(f) = 1/(1 + (f/f_{3\mathrm{dB}}^{(\mathrm{diode,eff})})^2)$, where $f_{3\mathrm{dB}}^{(\mathrm{diode,eff})}$ is the effective 3dB-frequency of the low-pass filter constituted by the position detection system. The 3dB-frequency, $f_{3\mathrm{dB}}^{(\mathrm{diode,eff})}$, is treated as a fitting parameter.

(ii) Often, the theoretical power spectrum is known for the case of infinite sampling frequency. The effect of a finite sampling frequency, *aka* aliasing, is easily accounted for, though. If filtering is also present, the filtered and aliased version of the theoretical power spectrum is

$$P^{(\mathrm{aliased})} = \sum_{n=-\infty}^{\infty} P^{(\mathrm{filtered})}(f + n f_{\mathrm{sample}}) \tag{7}$$

If filtering is not present, replace $P^{(\mathrm{filtered})}$ by $P^{(\mathrm{theory})}$ in Eq. (7).

Finally, drift may also result in systematic errors. But drift in the experimental setup happens at a time scale much longer than the interesting dynamics of the system studied, and thus shows in the low frequency part of the experimental power spectrum. Therefore, problems of drift can be accounted for simply by omitting the low frequency part of the experimental power spectrum when fitting one's theory (or filtered and aliased version of the theory) to $P^{(\mathrm{ex})}(f)$.

[b] In ref. 22 no assumptions about the underlying time series $x(t_i)$, are specified, however. We believe there must be some requirements.

All of the modifications described above have been applied to calibrate optical tweezers with a precision below 1% [19], and it has been suggested that a combination of precise measurements and the theory and tools of analysis put forward in Ref. 19 may lead to an experimental demonstration of the frequency dependence of thermal noise in liquids [24].

3. Subdiffusion in the cytoplasm of living yeast cells

The polymers of the cytoskeleton have been the subject of interest for a number of microrheological experiments using optical trapping and/or tracking. Actin-filament networks have been studied in *in vitro* experiments [25,26,27] and the viscoelastic properties of living cells have been studied in epithelial cells [28], in fibroblasts [29] and in fission yeast [30]. In these microrheological experiments, the characteristics of the viscoelastic medium is found from the stochastic motion of micronsized probe particles [31,32]. Here, we investigate whether the stochastic motion of the probe particles can be described by simple or anomalous diffusion.

3.1. *Biological system*

The main interest of our investigations is the nanomechanics of the cytoskeleton of the fission yeast *Schizosaccharomyces pombe*. This cytoskeleton consists of a sparse microtubule network [33] and actin filaments [34]. For quantitative *in vivo* measurements, however, the cytoplasm must first be characterized, and as alluded to above, we do so by studying probe particles embedded in the cytoplasm. Our probe particles are small lipid granules that occur naturally in the cytoplasm. The granules vary in size with a typical diameter of $\sim$300 nm, and they are highly refractive, almost spherical, and filled with lipids [35]. The whole cell is $\sim 12\,\mu$m long and $4\,\mu$m wide. For details of the experiment, consult Ref. 30.

3.2. *Optical tweezers measurements of subdiffusion of granules*

Theoretically, the mean squared displacement of a diffusing particle varies with time as $\mathrm{MSD}(t) \propto t^{\alpha}$, where α distinguishes the type of diffusion encountered; $\alpha = 1$ indicates normal Brownian diffusion, $0 < \alpha < 1$ subdiffusion, and $\alpha > 1$ superdiffusion [36,37]. The motion of a probe particle in a viscoelastic medium is described by a generalized Langevin equation with a time-dependent friction coefficient, and the power law variation $\mathrm{MSD(t)} \propto t^{\alpha}$ results in a similar power law in the theoretical power spectrum for the position of the probe particle:

$$P_{\mathrm{adiff}}(f) = k f^{-(1+\alpha)}; \tag{8}$$

This expression for the theoretical spectrum may be modified due to the presence of the optical trapping potential: For the model example discussed in section 2, where normal diffusion is encountered, the theoretical power spectrum is

$$P_{\mathrm{Lorentz}}(f) = \frac{D/(2\pi^2)}{f^2 + f_c^2}; \tag{9}$$

where $f_c = \kappa/(2\pi\gamma)$ is termed the *corner frequency*. It causes the power spectrum to "bend over" and approach a finite value as $f \to 0$. Within a viscoelastic medium (where $\alpha < 1$, typically), the presence of the optical trap alters the theoretical form for the power spectrum [38]. To lowest approximation, it gives rise to a similar "corner frequency factor" that adds to $f^{(1+\alpha)}$ in the denominator of $P_{\mathrm{adiff}}(f)$. In experiments in live *S. pombe*, a very weak optical trap was used, and as a result the corresponding corner frequency f_c was below 10 Hz. In the data analysis below, we consider frequencies above 200 Hz only, and we preferred to use Eq. (8) rather than adding the extra fitting parameter (f_c) that appear in the approximate expression.

In order to demonstrate normal diffusion of the granules in water, experiments where the cells were lysed were performed. In that case, a form similar to P_{Lorentz} was used, however changed such that the exponent on f in the denominator was $1 + \alpha$, with α a fitting parameter.

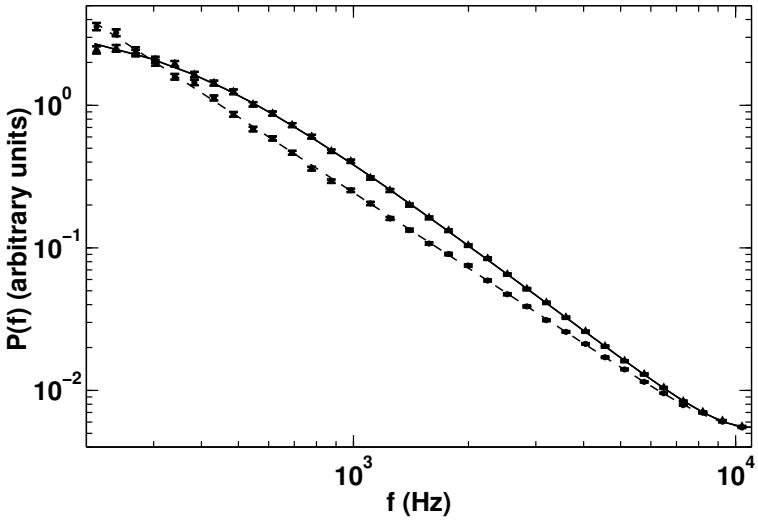

Fig. 1. Power spectra of the position of a trapped granule. Data plotted with filled circles and errorbars shows the power spectrum of positions of a granule in a living cell. The dashed line through the data is a fit of Eq. (8), filtered and aliased as in Eq. (7). The fit gave $\alpha = 0.762 \pm 0.006$. Data plotted with triangles and errorbars is the power spectrum of positions of a trapped granule in a cell that was lysed such that the granule moves in water. The solid curve going through the data is a fit where the presence of the optical trapping potential was accounted for. From this fit, we obtained the value $\alpha = 1.00 \pm 0.01$.

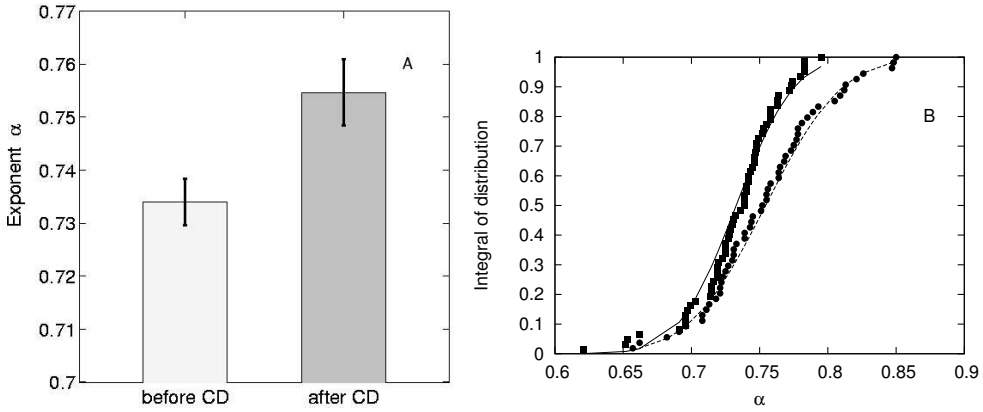

Fig. 2. Panel A: Change in α with addition of CD. See text for a discussion of the significance of the result. Error bars are standard error on the mean. Panel B: The integral of the distribution of α vs. α. Filled squares correspond to untreated cells and filled circles correspond to cells treated with CD. The lines through the data are the expected error-functions, see text.

The results presented in Fig. 1 are typical and in a population of cells, we found a mean value of the exponent of $\alpha = 0.734 \pm 0.004$ (59 granules, mean $\pm$ standard error on the mean).

This value of α is indicative for the motion of the granules at least over the timescale of a measurement. The sampling rate was 22 kHz and typically, a time series consisted of 2^{18} datapoints, yielding a total measurement time of 11.9 s. We do not believe that we are observing a transient phenomenon: If we assume that the cellular concentration of actin is of order 0.5 mg/ml[c], the average actin filament mesh size [39] is comparable to the size of the granules. Therefore, if transient diffusional properties would appear, we would expect those to show (closer to) normal diffusion on the shortest time scales. Also, we note that in experiments with a different detection apparatus, on a much longer time scale, we obtained similar values for α [30]. As the laser trap invokes a weak confinement of the granules, the finite size of the yeast cell does not influence our results either.

3.3. *Subdiffusion of granules with chemical disruption of actin networks*

What is causing the subdiffusive behavior? Our finding of $\alpha \sim 0.75$ resembles results from semi-dilute solutions of actin-networks [40,25]. Therefore, we performed experiments in which actin filaments in living cells were disrupted by Cytochalasin D (CD). The final concentration of CD in these experiments was 50 μM. If actin filaments restrict the motion of the granules, disruption of the actin network should induce a shift in the granule motion towards normal diffusion, which can be mea-

[c]This value originates from an analysis of elastic moduli, based on the results in Ref. 30

sured by an increase in α. In measurements on cells treated with CD, the data analysis gave $\alpha = 0.755 \pm 0.006$ (52 granules). The value of α measured in the same set of cells before treatment was $\alpha = 0.734 \pm 0.004$ (59 granules). Both values stated are the mean value and standard error on the mean. This is illustrated in Fig. 2. These values of α come from the fits with a goodness-of-fit [22] larger than 10%, which was the case for 89.9% of the total number of fits. The difference between the two values of α is roughly three times larger than the error on their difference. A Student's t-test [22] showed that the untreated and the CD-treated sample are signicantly different, i.e., that they could have the same mean with a probability $p < 0.01$. Since cell-to-cell variation in exponents is rather large, we also compared the mean exponent for each cell before and after the CD-treatment using a paired t-test [22], which yielded the same result ($p < 0.01$). Control experiments where cells were treated similarly but without CD did not show a significant change in α ($p = 0.4$).

Also shown in Fig. 2 is an integral over the distribution of values for the fitting parameter α. In the fitting procedure, we assumed that the distribution was Gaussian, thus the integrated distribution would be an error function. In the figure, the data are overlaid with the error function that corresponds to the average and standard deviation of the values of α found. This serve as additional demonstration of the conclusion that the distribution of values of α for normal cells and for cells treated with CD are different.

3.4. *Control experiments in* in vitro *actin solutions*

In a series of *in vitro* experiments in semi-dilute solutions of filamenteous actin, we investigated changes in α with increasing concentration of CD. The protocol for preparation of experimental samples is given in the appendix. We used an actin concentration of 2.5 mg/ml. Polystyrene beads with a diameter of 1 μm were added to a final concentration of 1:10000 and 25-30 μl was transferred to a test chamber composed of two microscope cover glasses separated by double sticky tape. The chamber was sealed with silicone grease.

A polystyrene bead was trapped by the optical tweezers, and time series of its position measured. Details of the experimental setup are given in Ref. 41. Power spectra were calculated and analysed, as in the case of granules within living yeast cells, Fig. 1. These data indicate that the variation of the fitted values of α increase linearly with [CD], from around 0.79±0.007 (151 beads) with no CD to 0.85±0.01 (34 beads) at a concentration of [CD]=100 μM, i.e. a somewhat larger increase than observed in the cells. The results are not directly comparable as we only have a rough estimate of the concentration of actin in the *in vivo* system of 0.5 mg/ml. It is clear, though, that with the 50 μM concentration of CD in the *in vivo* experiments, we should have measured a much larger increase in α if the actin filaments were the sole reason for subdiffusion of granules in the cytoplasm.

4. Conclusion

We have observed subdiffusion of granules in living cells of fission yeast. The granules occur naturally and the presence of laser light does not seem to harm the cells as they undergo division at their normal rate. Further, we have applied power spectral analysis and resolved a ∼3% change in the value of the subdiffusive exponent upon treatment of cells by actin-disrupting chemicals. This implies that within the cytoplasm of fission yeast, subdiffusion of granules is not mainly caused by the actin filaments, but rather the presence of other membraneous structures. Finally, in control *in vitro* experiments, a linear increase of α with [CD] was found. This is interesting as there is, to our knowledge, no theory that describes systems in the transition region between a semi-dilute solution of semi-flexible polymers and a purely viscous liquid.

Acknowledgments

We thank Genevieve Thon and Inga Sig-Nielsen for sharing their expertise on *S. pombe* with us. This work was supported by the Danish Research Councils, the Carlsberg Foundation and the Lundbeck Foundation.

Appendix A. Preparation of *in vitro* solution of filamenteous actin

2.5 mg freeze-dryed rabbit skeletal muscle actin (Sigma-Aldrich) was dissolved in 450 μl G-buffer [39]. 5 μl of polystyrene beads (Bangs Labs, diluted 1:100 in millipore water) were added, followed by 45 μl F-buffer [39] and mixed carefully, to reach an actin-concentration of 2.5 mg/ml. From this solution, samples were taken and CD, dissolved in F-buffer was added to achieve the concentration wanted. Samples were mixed for 60 minutes while being kept cold before the experiments were performed. In G-buffer, actin stays globular/monomeric, in F-buffer polymerization is induced.

References

1. Arthur Ashkin. Optical trapping and manipulation of neutral particles using lasers. *Proc. Natl. Acad. Sci. USA*, 94:4853–4860, 1997.
2. Steven Chu. The manipulation of neutral particles. *Rev. Mod. Phys.*, 70(3):685–706, 1998.
3. K C Neuman and S M Block. Optical trapping. *Rev. Sci. Ins.*, 75(9):2787–2809, 2004.
4. J.-C. Meiners and S. R. Quake. Femtonewton force spectroscopy of single extended DNA molecules. *Phys. Rev. Lett.*, 84:5014–5017, 2000.
5. M. J. Lang, C. L. Asbury, J. W. Shaevitz, and S. M. Block. An automated two-dimensional optical force clamp for single molecule studies. *Biophys. J.*, 83:491–501, 2002.
6. L Nugent-Glandorf and Perkins T T. Measuring 0.1-nm motion in 1ms in an optical microscope with differential back-focal-plane detection. *Opt. Lett.*, 29(22):2611–2613, 2004.
7. W J Greenleaf, M T Woodside, E A Abbondanzieri, and S M Block. Passive all-optical force clamp for high-resolution laser trapping. *Phys. Rev. Lett.*, 95(20):208102–1–4, 2005.

8. J R Moffitt, Y R Chemla, D Izhaky, and C Bustamante. Differential detection of dual traps improves the spatial resolution of optical tweezers. *Proc. Natl. Acad. Sci. USA*, 103(24):9006–9011, 2006.
9. E A Abbondanzieri, W J Greenleaf, J W Shaevitz, R Landick, and S M Block. Direct observation of base-pair stepping by RNA polymerase. *Nature*, 438(7067):460–465, 2005.
10. J. Liphardt, S. Dumont, S.B. Smith, I. Tinoco Jr., and C. Bustamante. Equilibrium information from nonequilibrium measurements in an experimental test of jarzynski's equality. *Science*, 296:1832–1835, 2002.
11. D Collin, F Ritort, C Jarzynski, S B Smith, I Tinoco, and C Bustamante. Verification of the crooks fluctuation theorem and recovery of RNA folding free energies. *Nature*, 437(7056):231–234, 2005.
12. J K Dreyer, K Berg-Sørensen, and L Oddershede. Quantitative approach to small-scale nonequilibrium systems. *Phys. Rev. E*, 73:051110–1–4, 2006.
13. I.M. Peters, Y. van Kooyk, S.J. van Vliet, B.G. de Grooth, C.G. Figdor, and J. Greve. 3d single-particle tracking and optical trap measurements on adhesion proteins. *Cytometry*, 36:189–194, 1999.
14. L. Oddershede, J. K. Dreyer, S. Grego, S. Brown, and K. Berg-Sørensen. The motion of a single molecule, the λ-receptor, in the bacterial outer membrane. *Biophys. J.*, 83:3152–3161, 2002.
15. L. Oddershede, H. Flyvbjerg, and K. Berg-Sørensen. Single-molecule experiment with optical tweezers: Improved analysis of the diffusion of the λ-receptor in *e.coli*'s outer membrane. *J. Phys.: Condens. Mat.*, 15:S1737–S1746, 2003.
16. K. Berg-Sørensen, L. Oddershede, and H. Flyvbjerg. Optical tweezers as a tool of precision: single-molecule mobility as case study. *Proceedings of SPIE*, 5322:64–74, 2004.
17. E.-L. Florin, A. Pralle, E. H. K. Stelzer, and J. K. H. Hörber. Photonic force microscope calibration by thermal noise analysis. *Appl. Phys. A*, 66:S75–S78, 1998.
18. K. Berg-Sørensen, L. Oddershede, E.-L. Florin, and H. Flyvbjerg. Unintended filtering in a typical photodiode detection system for optical tweezers. *J. Appl. Phys.*, 93:3167–3176, 2003.
19. Kirstine Berg-Sørensen and Henrik Flyvbjerg. Power spectrum analysis for optical tweezers. *Rev. Sci. Ins.*, 75:594–612, 2004.
20. Erwin J. G. Peterman, Meindert van Dijk, Lukas C. Kapitein, and Christoph F. Schmidt. Extending the bandwidth of optical-tweezers interferometry. *Rev. Sci. Ins.*, 74:3246, 2003.
21. Kirstine Berg-Sørensen, Erwin J. G. Peterman, Tom Weber, Christoph F. Schmidt, and Henrik Flyvbjerg. Power spectrum analysis for optical tweezers, II: Laser wavelength dependence of unintended filtering and how to achieve high band-width. *Rev. Sci. Ins.*, 77:063106, 2006.
22. W. H. Press, B. P. Flannery, S. A. Teukolsky, and W. T. Vetterling. *Numerical Recipes. The Art of Scientific Computing*. Cambridge University Press, Cambridge, 1986.
23. H. Flyvbjerg and H. G. Petersen. Error estimates on averages of correlated data. *J. Chem. Phys.*, 91:461–466, 1989.
24. K. Berg-Sørensen and H. Flyvbjerg. The color of thermal noise in classical brownian motion: A feasibility study of direct experimental observation. *New J. Phys.*, 7:38, 2005.
25. F. Gittes, B. Schnurr, P. D. Olmsted, F. C. MacKintosh, and C. F. Schmidt. Microscopic viscoelasticity: Shear moduli of soft materials determined from thermal fluctuations. *Phys. Rev. Lett.*, 79:3286–3289, 1997.

26. E. Helfer, S. Harlepp, L. Bourdieu, J. Robert, F. C. MacKintosh, and D. Chatenay. Microrheology of biopolymer-membrane complexes. *Phys. Rev. Lett.*, 85:457–460, 2000.
27. E. Helfer, S. Harlepp, L. Bourdieu, J. Robert, F. C. MacKintosh, and D. Chatenay. Viscoelastic properties of actin-coated membranes. *Phys. Rev. E*, 63:021904–1–021904–13, 2001.
28. S. Yamada, D. Wirtz, and S.C. Kuo. Mechanics of living cells measured by laser tracking microrheology. *Biophys. J.*, 78:1736–1747, 2000.
29. Y. Tseng, T. P. Kole, and D. Wirtz. Micromechanical mapping of live cells by multiple-particle-tracking microrheology. *Biophys. J.*, 83:3162–3176, 2002.
30. Iva Marija Tolić-Nørrelykke, Emilia-Laura Munteanu, Genevieve Thon, Lene Oddershede, and Kirstine Berg-Sørensen. Anomalous diffusion in living yeast cells. *Phys. Rev. Lett.*, 93:078102–1–4, 2004.
31. B. Schnurr, F. Gittes, F. C. MacKintosh, and C. F. Schmidt. Determining microscopic viscoelasticity in flexible and semiflexible polymer networks from thermal fluctuations. *Macromolecules*, 30:7781–7792, 1997.
32. F. Gittes and F. C. MacKintosh. Dynamic shear modulus of a semiflexible polymer network. *Phys. Rev. E*, 58:R1241–R1244, 1998.
33. I. M. Hagan. The fission yeast microtubule cytoskeleton. *J. Cell Sci.*, 111:1603–1612, 1998.
34. Jr. R. J. Pelham and F. Chang. Role of actin polymerization and actin cables in actin-patch movement in schizosaccharomyces pombe. *Nat. Cell Biol.*, 3:235–244, 2001.
35. C. F. Robinow and J. S. Hyams. General cytology of fission yeast. In *Molecular Biology of the Fission Yeast*, pages 273–330. Academic Press, Inc., 1989.
36. M. J. Saxton and K. Jacobson. Single particle tracking, applications to membrane dynamics. *Annu. Rev. Biophys. Biomol. Struct*, 26:3373–3399, 1997.
37. R. Metzler and J. Klafter. The random walk's guide to anomalous diffusion: A fractional dynamics approach. *Phys. Rep.*, 339:1–77, 2000.
38. M. Fischer and K. Berg-Sørensen. Calibration of optical tweezers in viscoelastic media, I: Method and simulation results. Preprint, 2006.
39. M. L. Gardel, M. T. Valentine, J. C. Crocker, A. R. Bausch, and D. A. Weitz. Microrheology of entangled F-actin solutions. *Phys. Rev. Lett.*, 91:158302, 2003.
40. F. Amblard, A. C. Maggs, B. Yurke, A. N. Pargellis, and S. Leibler. Subdiffusion and anomalous local viscoelasticity in actin networks. *Phys. Rev. Lett.*, 77:4470–4473, 1996.
41. L. Oddershede, S. Grego, S. F. Nørrelykke, and K. Berg-Sørensen. Optical tweezers: Probing biological surfaces. *Probe Microsc.*, 2:129–137, 2001.